

# Rotation estimation for a satellite from Sun sensors

Lionel Magnis

Nicolas Petit

**Abstract**—We develop a method to reconstruct the rotation motion of a satellite from Sun sensor measurements. Mathematically, the estimation objective is formulated as the problem of phase reconstruction for a 2-dimensional periodic function. A computationally straightforward solution is proposed. Theoretical developments allow to assess the robustness to model imperfections, sampling and noise. Simulation results illustrate practically obtainable performance..

## I. INTRODUCTION AND PROBLEM STATEMENT

Consider a satellite orbiting around the Earth in a region where its motion is governed by gravitational forces and actuators which generate its spin motion. The body frame of the satellite is assumed to rotate with respect to an inertial frame of reference such that the spin rotation is relatively slow but not negligible. The problem treated in this contribution is to estimate this spin motion from Sun sensors. This question is motivated by recent works [1] in the aerospace area. Typically envisioned cases of application encompass deployment of micro-satellite from the ISS (International Space Station), attitude monitoring of spin or dual-spin satellite, early detection and diagnosis of attitude instability, among others. While several estimation techniques have been considered earlier, including video processing, inertial navigation, magnetometry attitude determination [2], the data produced with these techniques have to be consolidated using another source of information. Sun sensors, which are commonly available [3], seem like a promising solution. Usually, the Sun sensors are used directly in the attitude determination to complement measurement from magnetometers [4], and star cameras [5], see also [6]. In this paper, we propose a method that uses the Sun sensors alone, in an innovative way.

The energy deposited in a photocell being proportional to the cosine of the angle of incidence of solar radiation, the output signal of a Sun sensor is, roughly speaking, a cosine function of this angle<sup>1</sup>. Yet, the cosine description model is incomplete [7], [8] as it does not account for sensor discrepancies (nonlinearities, noise) and various other effects (interferences, reflection from surrounding structures and celestial bodies among others).

To determine without any ambiguity the angular position of the Sun with respect to the satellite body frame and to guarantee all time visibility of the Sun, several sensors are

placed onto the rigid body. The approach we advocate in this article is to use the information arising from these several sensors, *simultaneously*, to reconstruct an estimate of the spin angle. Interestingly, the method does not use any other sensor such as gyrometer [9], gravimeter or accelerometer, and can therefore produce a stand-alone robust and redundant source of information for guidance, navigation and control purposes.

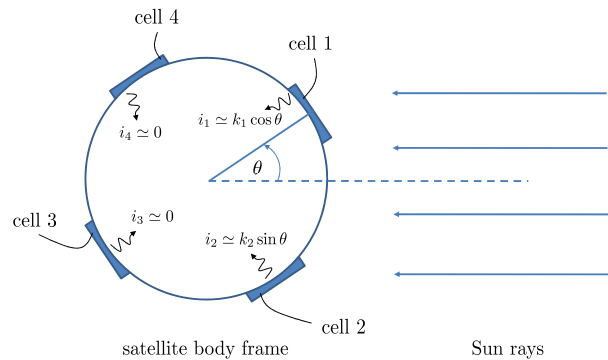


Fig. 1. For  $0 \leq \theta \leq \frac{\pi}{2}$ , photocells 3 and 4 lie in the shadow of the satellite. The output currents of photocells 1 and 2 are roughly proportional respectively to  $\cos \theta$  and  $\sin \theta$ .

In details, we consider a satellite equipped with four Sun sensors homogeneously distributed on its circumference and pointing (almost) orthogonal directions, see Fig. 1. At all times, exactly two sensors produce a nonzero signal (corrupted by noise) generated by the perceived sunlight, the other two sensors being in the shadow of the satellite. Typical signals are represented on Fig. 2.

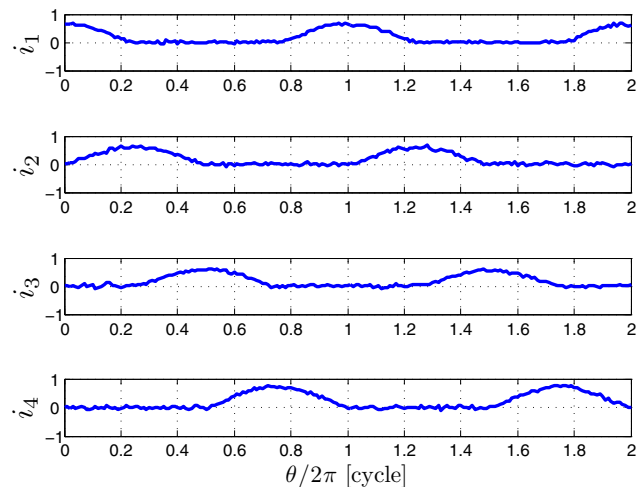


Fig. 2. Typical variation of the output current of the photocells with respect to the satellite orientation.

L. Magnis is a PhD candidate in Mathematics and Control at CAS, MINES ParisTech, 60 bd Saint-Michel, 75272 Paris Cedex FRANCE lionel.magnis@mines-paristech.fr

N. Petit is Professor at CAS, MINES ParisTech, 60 bd Saint-Michel, 75272 Paris Cedex FRANCE nicolas.petit@mines-paristech.fr

<sup>1</sup>for this reason, Sun sensors are frequently called cosine detectors

At a given time  $t$ , we note  $\theta(t)$  the rotation angle of the satellite with respect to a reference initially aligned with the Sun. The set of sensors provides two signals proportional respectively to  $\cos \theta(t)$  and  $\sin \theta(t)$ , up to the previously discussed model errors and nonlinearities. Instead of separately inverting the two measurements to get two independent estimates of  $\theta(t)$ , we propose the following approach. We gather the two signals in a single 2-dimensional vector and determine its argument (angle with respect to an axis of reference). This direct approach gives a straightforward solution to the problem under consideration, yet its implementation needs investigations, covering the various practical issues that can be expected and which are modeled here under the form of additive noise and sampling.

Mathematically, we recast the problem of estimating  $\theta(t)$  as the phase estimation of a 2-dimensional vector. Such a signal can be written as  $f(\theta(t))$ , where  $f$  is a  $2\pi$ -periodic complex function. The signal is sampled at frequency  $\nu_s = \frac{1}{\Delta t}$  and corrupted by the aforementioned noise. To sum up, we consider the following problem.

*Problem 1:* Knowing  $N$  measurements

$$y[k] = f(\theta[k]) + n[k] \in \mathbb{C}, \quad 1 \leq k \leq N \quad (\text{I.1})$$

where

- $f$  is an (unknown)  $2\pi$ -periodic function valued in  $\mathbb{C}$  (or equivalently in  $\mathbb{R}^2$ )
- $\theta[k] = \theta(k\Delta t)$  with  $\theta[1] = 0$
- $n[k]$  is a measurement noise

find an estimate  $\hat{\theta}[k]$  of  $\theta[k]$ .

The paper proposes a solution to this problem. It is organized as follows. In Section II, we first consider an idealized version of Problem 1 where no noise is present. Starting with a continuous phase description, and introducing sampling, we lay the basis of the solution method and provide a bound on the estimation error. In Section III, we take the noise into account and quantify its impact on the estimation algorithm. Solutions to Problem 1 are summarized and simulation results are provided in Section IV. Conclusions and perspectives are given in Section V.

## II. ESTIMATION PRINCIPLE

In this section we consider Problem 1 without any noise. We start by introducing some notations and defining the phase variation of  $f$  around an origin in section II-A. In section II-B we see how this phase variation gives an estimate of  $\theta$  as  $\theta$  varies continuously. Finally, we build the estimate of the sampled  $\theta[k]$  in Section II-C.

### A. Preliminaries and notations

We introduce handy notations and recall some basic complex analysis results (as exposed in details in [10] e.g.). The ambient space is the complex plane  $\mathbb{C}$  counterclockwise orientated, its origin is noted  $O$ .

We assume that  $f$  is  $C^1$ . For any  $\theta_1, \theta_2$ , we note  $\mathcal{C}_{[\theta_1, \theta_2]}$  the curve described by  $f(\varphi)$  for  $\varphi \in [\theta_1, \theta_2]$ .

The closed curve  $\mathcal{C}_{[0, 2\pi]}$  is simply noted  $\mathcal{C}$ . To simplify, we assume that  $\mathcal{C}$  is a Jordan curve, i.e. is non-self-intersecting. Thus, by the classic Jordan curve theorem,  $\mathcal{C}$  separates  $\mathbb{C}$  in two regions (connected components). We note  $\mathcal{I}$  the bounded one (i.e. interior).

For any  $\theta \in \mathbb{R}$  and any  $z_0 \in \mathbb{C} \setminus \mathcal{C}$ , the phase variation of  $f(\varphi)$  with respect to  $z_0$  as  $0 \leq \varphi \leq \theta$  is defined as:

$$R(\theta, z_0) = \Im \int_{\mathcal{C}_{[0, \theta]}} \frac{dz}{z - z_0} \triangleq \Im \int_0^\theta \frac{f'(\varphi)}{f(\varphi) - z_0} d\varphi \quad (\text{II.1})$$

where  $\Im$  designates the imaginary part. This definition is illustrated on Fig. 3. By definition,  $R(2\pi, z_0)$  is equal to  $2\pi I_{z_0}$ ,

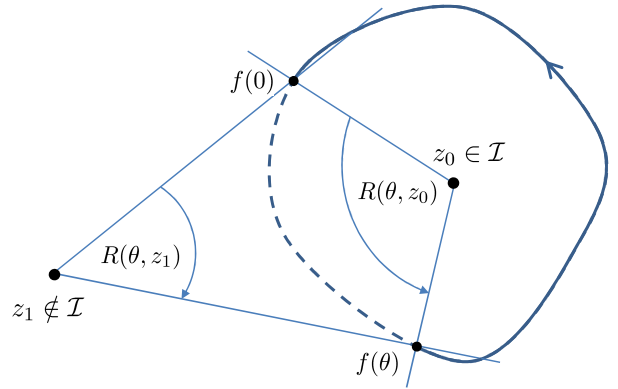


Fig. 3. Phase variations around origins  $z_0$  or  $z_1$  when  $f(\varphi)$  describes  $\mathcal{C}_{[0, \theta]}$ .

where  $I_{z_0} \in \mathbb{Z}$  is the algebraic number of counterclockwise rotation of  $\mathcal{C}$  around  $z_0$ . Namely,  $I_{z_0} \neq 0$  if and only if  $z_0 \in \mathcal{I}$ , and then it equals to 1 or  $-1$ . By assumption, we consider that  $I_{z_0} = 1$  for all  $z_0 \in \mathcal{I}$  throughout the paper, that is  $\mathcal{C}$  is positively oriented.

*Remark 1:* For an oriented segment  $[z_1, z_2]$  and  $z_0 \notin [z_1, z_2]$ , we have:

$$\Im \int_{[z_1, z_2]} \frac{dz}{z - z_0} = \arg_{-\pi} \frac{z_2 - z_0}{z_1 - z_0}$$

where  $\arg_{-\pi}$  designates the argument determination in  $]-\pi; \pi[$ . We will abundantly use this result in the following.

### B. Estimate of a continuous phase

We take  $z_0 \in \mathcal{I}$ . We will see that  $R(\theta, z_0)$  gives an estimate of  $\theta$  under some assumptions on  $f$ . For now, let us note the estimation error

$$e_{z_0}(\theta) = R(\theta, z_0) - \theta \quad (\text{II.2})$$

and derive bound for it. Let  $\{c_n\}_{n \in \mathbb{Z}}$  be the coefficients of the Fourier expansion of  $f$ . We define

$$g(\varphi) \triangleq \exp(-i\varphi) (f(\varphi) - z_0)$$

which gives

$$g(\varphi) = c_1 + \sum_{n \neq 0, 1} c_n e^{i(n-1)\varphi} + (c_0 - z_0) e^{-i\varphi}$$

Using this new function, we can directly prove the following result.

*Proposition 1:* For any  $z_0 \in \mathcal{I}$ ,

$$e_{z_0}(2n\pi) = 0, \quad \forall n \in \mathbb{Z} \quad (\text{II.3})$$

and  $e_{z_0}(\theta)$  is bounded by:

$$|e_{z_0}|_\infty = \max_{0 \leq \varphi \leq 2\pi} \left| \Im \int_0^\varphi \frac{g'(\tau)}{g(\tau) - z_0} d\tau \right| \quad (\text{II.4})$$

*Proof:* For any  $\theta \in \mathbb{R}$ , we have

$$\begin{aligned} R(\theta, z_0) &= \Im \int_0^\theta \left( i + \frac{g'(\varphi)}{g(\varphi)} \right) d\varphi \\ &= \theta + \Im \int_0^\theta \frac{g'(\tau)}{g(\tau) - z_0} d\tau \end{aligned}$$

For the particular value  $\theta = 2\pi$ , the last integral equals zero. Then, using this fact, for any  $\theta = 2n\pi + \varphi$  with  $n \in \mathbb{Z}$  and  $0 \leq \varphi \leq 2\pi$ , we directly get

$$e_{z_0}(\theta) = \Im \int_0^\varphi \frac{g'(\tau)}{g(\tau) - z_0} d\tau$$

The result follows immediately.  $\blacksquare$

Equation (II.3) means that the estimate matches  $\theta$ , at least once every cycle. The error bound (II.4) is of theoretical but not of practical value. To derive more concrete bounds, we need to make further assumptions on  $g$ .

Let us assume that there exists  $r < |c_1|$  such that the set  $\{g(\varphi), \varphi \in [0; 2\pi]\}$  lies in the closed circle  $D(c_1, r)$  of center  $c_1$  and radius  $r$ . Then, as is illustrated in Fig. 4, for any  $\varphi$  the angle  $\angle g(0)Og(\varphi)$  is included in  $\angle AOB$ , whose value is  $2 \arcsin \frac{r}{|c_1|}$ . Thus,  $e_{z_0}(\theta)$  is bounded by

$$|e_{z_0}|_\infty \leq 2 \arcsin \frac{r}{|c_1|}$$

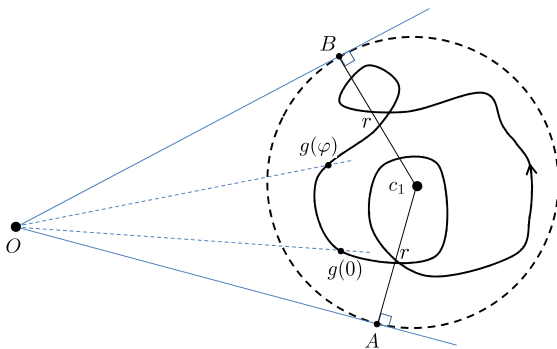


Fig. 4. Bound on the estimation error when  $O$  lies outside a disk containing the curve of  $g$

This inequality allows us to directly derive the following result, obtained with  $r = |g - c_1|_\infty$

*Proposition 2:* If  $f$  is such that its Fourier expansion satisfies

$$|c_1| > \sum_{n \neq 0, 1} |c_n| + |c_0 - z_0| \quad (\text{II.5})$$

then one has

$$|e_{z_0}|_\infty \leq 2 \arcsin \frac{\sum_{n \neq 0, 1} |c_n| + |c_0 - z_0|}{|c_1|} \quad (\text{II.6})$$

*Example 1:* Let us consider a positively oriented ellipse with eccentricity  $e$  between 0 and 1

$$f(\theta) = A \cos \theta + i\sqrt{1 - e^2} A \sin \theta$$

In this case,  $f$  has only two Fourier coefficients

$$\begin{aligned} c_1 &= \frac{1 + \sqrt{1 - e^2}}{2} A \\ c_{-1} &= \frac{1 - \sqrt{1 - e^2}}{2} A \end{aligned}$$

As  $0 < c_{-1} < c_1$ , condition (II.5) is met for  $z_0 = O$  and we have the bounded error

$$|e_O|_\infty \leq 2 \arcsin \frac{1 - \sqrt{1 - e^2}}{1 + \sqrt{1 - e^2}} = \frac{e^2}{2} + O(e^4)$$

Even for a flat ellipse with  $e = 0.99$ , this estimation error does not exceed  $\frac{1}{4}$ -cycle.

The method we developed in this section provides an estimate of  $\theta$ , assuming we can compute *i*) an origin  $z_0 \in \mathcal{I}$ , *ii*) the integral term (II.1). The latter problem will be addressed in the next section. The choice of an origin can be a difficult problem. It is investigated in Section III.

### C. Estimate from samples

We now consider the case of discrete time measurements, a *noise-less* version of Problem 1. To estimate  $\theta[k]$ , we will apply the preceding method, to the polygonal line joining the vertices  $f(\theta[1]) \dots f(\theta[k])$ , which are measured. The case of noisy measurements will be considered later in Section III. Here, we will see that the integral term (II.1) can still be exactly evaluated at each sampling time  $\theta[k]$  thanks to a direct formula. To formalize this, let us first introduce a few notations specific to this section.

For any  $1 \leq k \leq N - 1$ , we simply note  $\tilde{\gamma}_k = \mathcal{C}_{[\theta[k], \theta[k+1]]}$  and  $\gamma_k$  the oriented segment  $[f(\theta[k+1]), f(\theta[k])]$ , so that the concatenation  $\gamma_k \cdot \tilde{\gamma}_k$  is a closed curve. We also note  $\Omega_k$  the unbounded region defined by this closed curve. These notations are illustrated in Fig. 5.

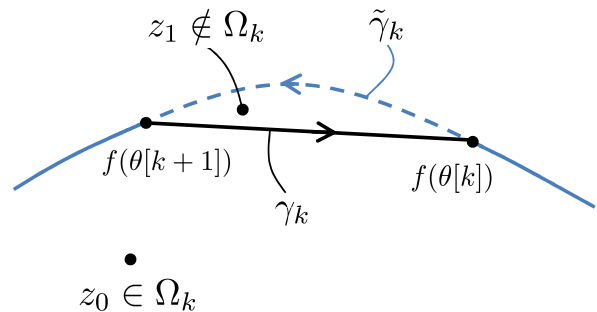


Fig. 5. Curves  $\gamma_k$  and  $\tilde{\gamma}_k$

The next result states that, if  $z_0$  is chosen in the intersection of all the  $\Omega_k$ , integral (II.1) can be calculated from the sampled values.

*Proposition 3:* Assuming that  $z_0$  satisfies

$$z_0 \in \bigcap_{k=1}^{N-1} \Omega_k \cap \mathcal{I} \quad (\text{II.7})$$

then for all  $2 \leq k \leq N$ ,

$$R(\theta[k], z_0) = \sum_{j=1}^{k-1} \arg_{-\pi} \frac{f(\theta[j+1]) - z_0}{f(\theta[j]) - z_0} \quad (\text{II.8})$$

*Proof:* Let  $k$  be any  $1, \dots, N-1$ . The condition  $z_0 \in \Omega_k$  implies that:

$$0 = \Im \int_{\gamma_k} \frac{dz}{z - z_0} + \Im \int_{\bar{\gamma}_k} \frac{dz}{z - z_0}$$

Using the formula recalled in Remark 1, we have

$$\Im \int_{\bar{\gamma}_k} \frac{dz}{z - z_0} = -\Im \int_{\gamma_k} \frac{dz}{z - z_0} = \arg_{-\pi} \frac{f(\theta[k+1]) - z_0}{f(\theta[k]) - z_0}$$

Similarly, for  $2 \leq k \leq N$ , the calculus above is generalized to

$$R(\theta[k], z_0) = \sum_{j=1}^{k-1} \Im \int_{\bar{\gamma}_j} \frac{dz}{z - z_0} = \sum_{j=1}^{k-1} \arg_{-\pi} \frac{f(\theta[j+1]) - z_0}{f(\theta[j]) - z_0}$$

Now the definition of our estimate directly follows. For any  $2 \leq k \leq N$ , and any  $z_0 \in \mathbb{C}$ , we define the estimate  $\hat{\theta}_{z_0}[k]$  as

$$\hat{\theta}_{z_0}[k] = \sum_{j=1}^{k-1} \arg_{-\pi} \frac{y[j+1] - z_0}{y[j] - z_0} \quad (\text{II.9})$$

and the estimate error  $e_{z_0}[k]$  as

$$e_{z_0}[k] = \hat{\theta}_{z_0}[k] - \theta[k] \quad (\text{II.10})$$

Proposition 3 formulated above guarantees that, *in the absence of noise* i.e.  $n[k] = 0$  for  $1 \leq k \leq N$ , the estimate error is exactly  $e_{z_0}[k] = e_{z_0}(\theta[k])$ . Hence, the bounds on  $e_{z_0}$  listed in Section II-B still apply on  $e_{z_0}[k]$ .

### III. IMPACT OF MEASUREMENT NOISE

#### A. Critical value of the noise magnitude

We now consider Problem 1 in its full version, i.e. with noise. For any  $1 \leq k \leq N-1$ , we note  $Q_k$  the (non necessarily convex) quadrilateral with ordered vertices  $f(\theta[k])$ ,  $y[k]$ ,  $y[k+1]$ ,  $f(\theta[k+1])$ . The next result provides a bound on the error estimate, provided  $z_0$  is taken outside all the  $Q_k$ .

*Proposition 4:* Assuming that  $z_0$  satisfies condition (II.7) and

$$z_0 \notin Q_k, \forall k \in \{1, \dots, N-1\} \quad (\text{III.1})$$

then for all  $2 \leq k \leq N$ ,

$$\begin{aligned} e_{z_0}[k] &= e_{z_0}(\theta[k]) + \arg_{-\pi} \frac{y[k] - z_0}{f(\theta[k]) - z_0} \\ &\quad - \arg_{-\pi} \frac{y[1] - z_0}{f(\theta[1]) - z_0} \end{aligned} \quad (\text{III.2})$$

*Proof:* For any  $1 \leq k \leq N-1$ , note

- $\gamma_k^n$  the oriented segment  $[f(\theta[k]), y[k]]$ , and  $\gamma_k^{n-}$  the opposed oriented segment  $[y[k], f(\theta[k])]$
- $\bar{\gamma}_k$  the oriented segment  $[y[k], y[k+1]]$

These notations are illustrated in Fig. 6.

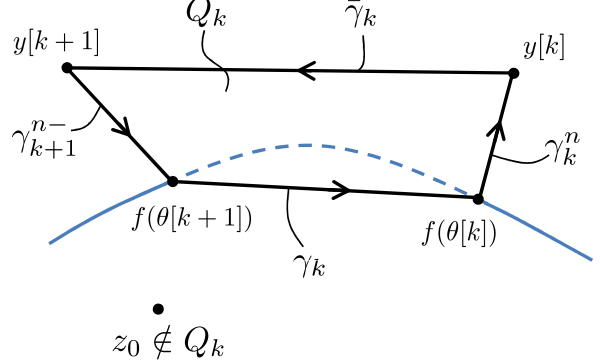


Fig. 6.  $Q_k$ 's boundary is the closed curve  $\gamma_k^n \cdot \bar{\gamma}_k \cdot \gamma_{k+1}^{n-} \cdot \gamma_k$

As  $z_0 \notin Q_k$ , we have

$$\begin{aligned} 0 &= \int_{\gamma_k^n} \frac{dz}{z - z_0} + \int_{\bar{\gamma}_k} \frac{dz}{z - z_0} \\ &\quad + \int_{\gamma_{k+1}^{n-}} \frac{dz}{z - z_0} + \int_{\gamma_k} \frac{dz}{z - z_0} \end{aligned}$$

Let us now consider  $k \in \{2, \dots, N\}$  and sum the terms of this equation for  $1 \leq j \leq k-1$ . This gives

$$\begin{aligned} 0 &= \int_{\gamma_1^n} \frac{dz}{z - z_0} + \int_{\bar{\gamma}_1 \dots \bar{\gamma}_{k-1}} \frac{dz}{z - z_0} \\ &\quad + \int_{\gamma_k^{n-}} \frac{dz}{z - z_0} + \int_{\gamma_1 \dots \gamma_{k-1}} \frac{dz}{z - z_0} \end{aligned}$$

Integrating  $\frac{dz}{z - z_0}$  on the polygonal lines and taking the imaginary part of the obtained result, we get

$$\begin{aligned} \hat{\theta}_{z_0}[k] &= \sum_{j=1}^{k-1} \arg_{-\pi} \frac{f(\theta[j+1]) - z_0}{f(\theta[j]) - z_0} + \arg_{-\pi} \frac{y[k] - z_0}{f(\theta[k]) - z_0} \\ &\quad + \arg_{-\pi} \frac{y[1] - z_0}{f(\theta[1]) - z_0} \end{aligned}$$

Under the formulated assumption (III.1), we have

$$\sum_{j=1}^{k-1} \arg_{-\pi} \frac{f(\theta[j+1]) - z_0}{f(\theta[j]) - z_0} = e_{z_0}(\theta[k]) + \theta[k]$$

The result follows immediately. ■

We want to define a set of allowed origins in the sense of (II.7) and (III.1) independent of the values of  $\theta[k]$ . To do so, we introduce  $\rho$  the maximum noise amplitude and  $\Delta$  the maximum  $\theta$  variation between two consecutive samples such that for all  $k$ ,  $|y[k] - f(\theta[k])| \leq \rho$  and  $|\theta[k+1] - \theta[k]| \leq \Delta$ . It is assumed that  $\Delta < \pi$ .



*Proposition 6:* If  $\mathcal{I}$  is a convex set, we have

$$\mathcal{A}_{\rho,\Delta} = \mathcal{I} \cap \bigcap_{\theta=0}^{2\pi} \{z \in \mathbb{C}, \Re v^*(\theta)(z - f(\theta)) > \rho\} \quad (\text{III.6})$$

In particular,  $\mathcal{A}_{\rho,\Delta}$  is also a convex set.

*Proof:* The proof uses the same tools as the one of Proposition 5 and is omitted for brevity purposes. ■

Formula (III.6) helps us better understand the set of allowed origins. In particular, one can show that it inherits the axial symmetry properties of  $f$ . If  $f$  has two axis of symmetry, thus a center  $C$  at their intersection, and if the convex set  $\mathcal{A}_{\rho,\Delta}$  is not empty, then it contains  $C$ . Thus, a simple criteria on  $(\rho, \Delta)$  for  $\mathcal{A}_{\rho,\Delta}$  to be not empty is that  $C$  satisfies

$$\Re v(\theta)^*(C - f(\theta)) > \rho, \forall \theta$$

For example, if  $f$  describes a circle of radius  $A$ , we easily deduce that  $\mathcal{A}_{\rho,\Delta}$  is not empty if and only if  $\rho < A \cos \frac{\Delta}{2}$ . More generally for the ellipse of Example 1, the criteria becomes  $\rho < A\sqrt{1 - e^2} \cos \frac{\Delta}{2}$ .

Let us now assume that  $\mathcal{A}_{\rho,\Delta}$  is not empty and that  $\mathcal{I}$  is strictly convex. Thus, the phase of  $v(\theta)$  is strictly increasing with  $\theta$  and  $(v(\theta), v'(\theta))$  is a direct frame of the plane. Namely,  $\Im v(\theta)^* v'(\theta) > 0$ .  $\mathcal{A}_{\rho,\Delta}$  is also strictly convex and its boundary can be derived from its tangent lines. Therefore, it is included in (but not necessarily equal to)  $\bigcup_{\theta=0}^{2\pi} \lim_{\delta\theta \rightarrow 0, \delta\theta \neq 0} \mathcal{D}_\theta^+ \cap \mathcal{D}_{\theta+\delta\theta}^+$ . The next result gives an explicit expression of this boundary.

*Proposition 7:* If  $\mathcal{A}_{\rho,\Delta}$  is not empty and  $\mathcal{I}$  is strictly convex, then  $\mathcal{A}_{\rho,\Delta}$  is an interior region defined by the (not necessarily Jordan) closed curve

$$h : [0, 2\pi] \ni \theta \mapsto f(\theta) + \rho v(\theta) + i \frac{\Re v(\theta)^* f'(\theta)}{|v'(\theta)|} v(\theta) \quad (\text{III.7})$$

*Proof:* Let  $\theta$  be in  $[0, 2\pi]$ . For  $\delta\theta \neq 0$  sufficiently small,  $v(\theta)$  and  $v(\theta + \delta\theta)$  are independent, namely  $\Im v^*(\theta)v(\theta + \delta\theta) \neq 0$ . Thus  $\mathcal{D}_\theta^+$  and  $\mathcal{D}_{\theta+\delta\theta}^+$  intersect on a unique point  $z(\theta, \theta + \delta\theta)$ , solution of

$$\Re v(\theta)^*(z - f(\theta)) = \rho = \Re v(\theta + \delta\theta)^*(z - f(\theta + \delta\theta))$$

which gives

$$\begin{aligned} z(\theta, \theta + \delta\theta) &= f(\theta) + \rho v(\theta) \\ &+ i \frac{\Re v(\theta)^*(f(\theta + \delta\theta) - f(\theta))}{\Im v(\theta)^*v(\theta + \delta\theta)} v(\theta) \\ &+ i \frac{\Re v(\theta)^*(v(\theta + \delta\theta) - v(\theta))}{\Im v(\theta)^*v(\theta + \delta\theta)} \rho v(\theta) \end{aligned}$$

We have  $\Im v(\theta)^*v(\theta + \delta\theta) = \Im v(\theta)^*v'(\theta)\delta\theta + o(\delta\theta)$ . Differentiating  $v(\theta)^*v(\theta) = 1$  gives  $\Re v(\theta)^*v'(\theta) = 0$  and  $\Im v(\theta)^*v'(\theta) = |v'(\theta)| \neq 0$ . Hence, we have

$$z(\theta, \theta + \delta\theta) = h(\theta) + o(\delta\theta)$$

Thus,  $\lim_{\delta\theta \rightarrow 0, \delta\theta \neq 0} \mathcal{D}_\theta^+ \cap \mathcal{D}_{\theta+\delta\theta}^+ = h(\theta)$ , which concludes the proof. ■

*Example 3:* If  $f$  represents a circle  $f(\theta) = Ae^{i\theta}$  and if  $\rho < A \cos \frac{\Delta}{2}$ , formula (III.7) gives

$$h(\theta) = (\cos \frac{\Delta}{2} - \rho)e^{i(\theta + \frac{\Delta}{2})}$$

Thus,  $\mathcal{A}_{\rho,\Delta}$  is the open disk of center  $O$  and radius  $\cos \frac{\Delta}{2} - \rho$ .

### C. Practical determination of an origin

We focus on the case of an ellipse, which is relevant for the problem under consideration. The best choice for an origin would be the ellipse center  $C$ . A practical difficulty is that the parameters of the ellipse are not directly given by the sampled noisy measurements. One simple alternative is to chose the mean of the measurements to average the noise contribution to zero. Though this solution is easy to implement, it might reveal troublesome as the average of the samples can be very different from  $C$  (thus not in  $\mathcal{A}_{\rho,\Delta}$ ). The culprit can be that the  $f(\theta[k])$  values may be not homogeneously distributed on the ellipse. One way to circumvent this problem is to compute an origin that only depends on the shape of the samples, disregarding potential aggregate of values. For example, we can try to compute a point as far as possible from the polygonal line drawn by the values  $y[k]$ , namely its Chebychev center.

Note  $\Gamma_k$  the polygon of ordered vertices  $y[1], \dots, y[k], y[1]$ . If  $\Gamma_k$  is convex, one can compute the Chebychev center of  $\Gamma_k$  with convex optimization methods. If not, the task is more difficult. We propose to pick a subset of  $y[1], \dots, y[k]$ , say  $z_1, \dots, z_{n_k}$  so that the polygon line  $\tilde{\Gamma}_k$  of ordered vertices  $z_1, \dots, z_{n_k}$  is convex and so that its shape reflects the one of  $\Gamma_k$ . For example, one could chose  $\tilde{\Gamma}_k$  as the convex hull of  $\Gamma_k$ . An other way could be to compute the largest convex polygon included in the set  $y[1], \dots, y[k]$ . Still another way could be to consider not the Chebychev center but the gravity center of the polygonal  $\tilde{\Gamma}_k$  (centroid). In this article we illustrate the first solution and we call Chebychev center of  $\Gamma_k$  the Chebychev center of its convex hull.

On Fig. 8, we simulated a non homogeneous  $\theta[k]$  distribution around a circle, with  $\rho = 1$ .  $\Delta$  is computed as the largest  $|\theta[k+1] - \theta[k]|$ .

## IV. SUMMARY OF RESULTS AND SIMULATION EXPERIMENTS

To summarize, we can now formulate the following results for Problem 1.

*Solution 1:* Consider Problem 1. Assume that  $f$  is such that its Fourier expansion  $\{c_n\}_{n \in \mathbb{Z}}$  satisfies

$$|c_1| > \sum_{n \neq 0, 1} |c_n| + |c_0 - z_0|$$

Assume that the interior region  $\mathcal{I}$  defined by the boundary  $C$  is strictly convex. Assume that the noise  $n$  is (uniformly) bounded by  $\rho$  and that  $|\theta[k+1] - \theta[k]|$  is (uniformly) bounded by  $\Delta < \pi$ . Then consider

$$\mathcal{A}_{\rho,\Delta} = \mathcal{I} \cap \bigcap_{\theta=0}^{2\pi} \{z \in \mathbb{C}, \Re v^*(\theta)(z - f(\theta)) > \rho\}$$

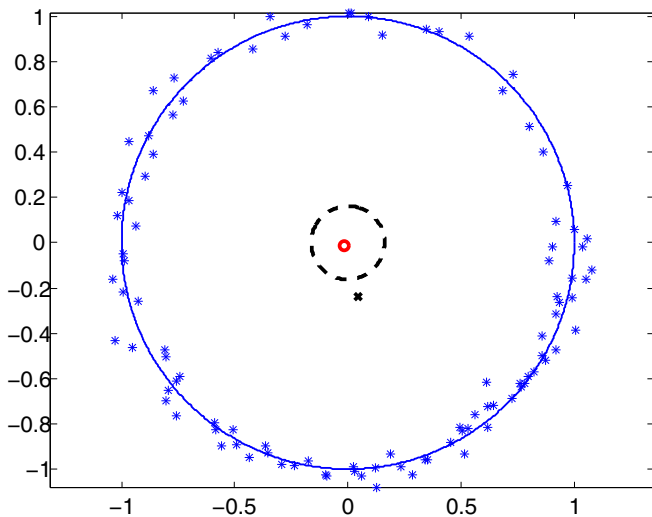


Fig. 8. The Chebychev center position (bubble) does not depend on the points distribution, but rather on the geometric shape of the samples. Therefore, it remains in the allowed origins set, while the average (cross) is dragged out by a non homogeneous distribution of the  $\theta[k]$ .

where  $v(\theta) = e^{+i\pi/2} \frac{f(\theta+\Delta) - f(\theta)}{|f(\theta+\Delta) - f(\theta)|}$ . If  $\mathcal{A}_{\rho, \Delta}$  is not empty, then the following sequence

$$\hat{\theta}_{z_0}[k] = \sum_{j=1}^{k-1} \arg_{-\pi} \frac{y[j+1] - z_0}{y[j] - z_0} \quad (\text{IV.1})$$

where  $z_0 \in \mathcal{A}_{\rho, \Delta}$  provides an estimate of  $\theta[k]$  with an error that is bounded by

$$|e_{z_0}|_{\infty} \leq 2 \arcsin \frac{\sum_{n \neq 0, 1} |c_n| + |c_0 - z_0|}{|c_1|} + 2 \arcsin \frac{\rho}{d(z_0)}$$

where  $d(z_0) = \min_{\varphi} |f(\varphi) - z_0|$ . In practice, a recommendation is to select  $z_0$  as one of the following: *i*) the Chebychev center of measurements, *ii*) the polygon centroid.

*Solution 2 (particular case of an ellipse):* Assume that  $f$  defines an ellipse  $f(\theta) = C + A \cos \theta + i\sqrt{1 - e^2} A \sin \theta$ . Consider  $\rho$  and  $\Delta$  as defined in Solution 1. Then  $\mathcal{A}_{\rho, \Delta}$  is not empty if and only if  $\rho < A\sqrt{1 - e^2} \cos \frac{\Delta}{2}$  and for  $z_0$  in  $\mathcal{A}_{\rho, \Delta}$ , (IV.1) gives an estimate of  $\theta[k]$ . For  $z_0 = C$ , the error is bounded by

$$|e_C|_{\infty} \leq 2 \arcsin \frac{1 - \sqrt{1 - e^2}}{1 + \sqrt{1 - e^2}} + 2 \arcsin \frac{\rho}{A\sqrt{1 - e^2}}$$

To illustrate these results, we now perform simulations using typical satellite photocells output as shown in Introduction. We consider the satellite initially at rest during a burst–burst manoeuvre. For  $t \in [0, 3]$ ,  $\ddot{\theta}(t) = 1$ , for

TABLE I

STANDARD DEVIATION OF THE ERROR ESTIMATE FOR VARIOUS SNR AND VARIOUS SAMPLING RATES.

	$\nu_s = 100$ Hz	$\nu_s = 50$ Hz	$\nu_s = 10$ Hz
$SNR = 30$ dB	$\sigma = 5.7^\circ$	$\sigma = 6.3^\circ$	$\sigma = 6.5^\circ$
$SNR = 13$ dB	$\sigma = 14.2^\circ$	$\sigma = 13.5^\circ$	$\sigma = 14.4^\circ$
$SNR = 5$ dB	$\sigma = 24.5^\circ$	$\sigma = 23.8^\circ$	$\sigma = 22.9^\circ$

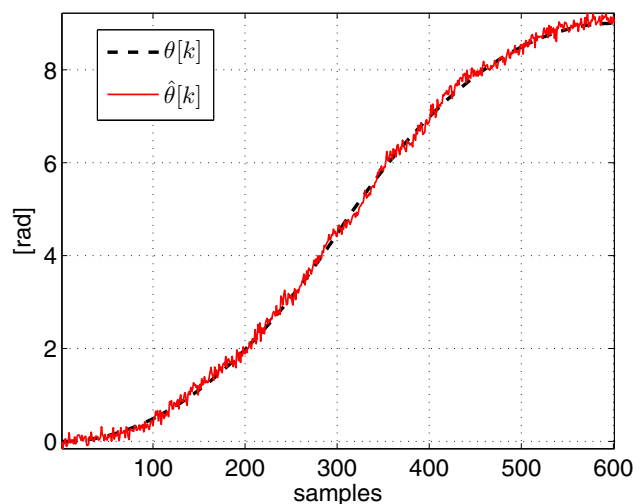


Fig. 9.  $\hat{\theta}[k]$  matches  $\theta[k]$  from the start to the end of the manoeuvre.

$t \in [3, 6]$ ,  $\ddot{\theta}(t) = -1$ . We consider several sampling rates ranging from 10 Hz to 100 Hz and SNR ranging from 5 dB to 30 dB. Typical results are pictured in Fig. 9. Numerical results are presented in Table I. As expected the estimate error grows with the noise amplitude. The sampling rate however does not seem to affect the error standard deviation.

It appears that the angle  $\theta$  is well estimated and that the spin motion of the satellite is relatively accurately estimated, enabling monitoring strategies. Post filtering of the estimate can also be used on-line or off-line (to avoid filtering lag) to smooth out visible artefacts. To obtain the presented results, the Chebychev center of the samples was computed only once, using linear programming techniques with an interior point method. Alternatively, the centroid point could be used, which reveals significantly lighter in terms of computational effort. The estimation algorithm itself consists in simple arithmetic operations, as detailed in Solution 1. No pre-filtering of data was employed.

## V. CONCLUSIONS AND PERSPECTIVES

We have studied a simple estimation procedure to reconstruct the phase of a 2-dimensional vector data representing periodic dynamics. The underlying idea stems from the classic notion of index of a curve and relates to the mathematics of complex and curve analysis. The application of the method to real data naturally raises the problem of noise and sampling. These issues have been treated by careful analysis, and sufficient conditions have been proposed to guarantee that the estimation is not jeopardized. Explicit bounds have been found for the error estimate. A critical notion of the proposed approach is the definition of suitable or *allowed origins*. Necessary conditions on noise level and on sampling rate have been derived to guarantee their existence. These conditions can be made explicit for the particular case of an ellipse, which is a natural approximation for numerous real situations. Derivating these conditions is the main theoretical result of this paper. In the future, our effort will be focused on the Chebychev center. It has proven

to be a good candidate as origin. Determining its value can be performed using standard numerical procedure. This could probably be improved in terms of computational burden. Besides, it is desirable to exploit its stochastic properties as one can expect that, when  $N$  grows, the Chebychev center tends to the set of suitable origins.

Alternative methods to solve the considered problem are phaselock loops [11]. They are the reference solution for frequency modulated signals, their most striking property being that they operate under very poor SNR. They are however sensitive to the phase dynamics. Our method, which is purely geometric is (relatively) independent on the phase dynamics. For these reasons, the two methods appear to be very complementary as they produce good performance under different operating conditions. Exploiting this complementarity is also a point for further investigations.

#### REFERENCES

- [1] B. Bruninga. Determining the attitude and rotation rate of atmospheric neutral density experiment. Technical report, US Naval Academy Satellite Lab., 2007.
- [2] T. Bak. *Spacecraft attitude determination - a magnetometer approach*. PhD thesis, Aalborg University, 1999.
- [3] J. M. Hall and M. Harris. Spacecraft Sun sensors. Technical report, NASA, 1970.
- [4] A. Kutlu, Ch. Hacıyev, and O. Tekinalp. Attitude determination and rotational motion parameters identification of a LEO satellite through magnetometer and sun sensor data. In *Recent Advances in Space Technologies, 2007. RAST '07. 3rd International Conference on*, pages 458 –461, june 2007.
- [5] A. Khosravian and M. Namvar. Rigid body attitude control using a single vector measurement and gyro. *Automatic Control, IEEE Transactions on*, 57(5):1273 –1279, 2012.
- [6] D. Choukroun. *Novel methods for attitude determination using vector observations*. PhD thesis, Technion, 2003.
- [7] W. J. Larson and J. R. Wertz. *Space mission analysis and design*. Microcosm, 1992.
- [8] Y. Winetraub, S. Bitan, Y. Nativ, and A. B. Heller. Attitude determination advanced sun sensors for pico-satellites. In *17th European Union Contest for Young Scientists, Moscow, Russia, Sep. 2005*, 2005.
- [9] G. Falbel and M. A. Paluszek. An ultra low weight/low cost three axis attitude readout system for nano-satellites. In *Aerospace Conference, 2001, IEEE Proceedings.*, volume 5, pages 2469 –2481 vol.5, 2001.
- [10] W. Rudin. *Real and complex analysis*. International series in pure and applied mathematics. McGraw-Hill, 1986.
- [11] F. M. Gardner. *Phaselock techniques*. Wiley, 3<sup>rd</sup> edition, 2005.